Functional Regulation of Sugar Assimilation by N-Glycan-specific Interaction of Pancreatic α-Amylase with Glycoproteins of Duodenal Brush Border Membrane*□[S]

Kimie Asanuma-Date[‡], Yuki Hirano[‡], Na Le[‡], Kotone Sano[‡1], Nana Kawasaki[§], Noritaka Hashii[§], Yoko Hiruta[§], Ken-ichi Nakayama[¶2], Mariko Umemura[¶3], Kazuhiko Ishikawa[¶4], Hiromi Sakagami[‡], and Haruko Ogawa[‡5]

From the [‡]Graduate School of Humanities and Sciences and the Glycoscience Institute, Ochanomizu University, 2-1-1 Otsuka, Bunkyo-ku, Tokyo 112-8610, the [§]Division of Biological Chemistry and Biologicals, National Institute of Health Sciences, Setagaya-ku, Tokyo 158-8501, and the [¶]National Institute of Advanced Industrial Sciences and Technology, 1-1-1 Higashi, Tsukuba, Ibaraki 305-8566, Japan

Background: PPA binds to specific glycoprotein N-glycans.
Results: Interaction between PPA and glycoligands in duodenum BBM activates glucose production while inhibiting glucose absorption by enterocytes.
Conclusion: N-Glycans in BBM function as a target for α-amylase in order to control glucose assimilation via their interaction.
Significance: We have discovered the modulatory role of BBM glycoprotein N-glycans, which contribute to blood glucose homeostasis.

Porcine pancreatic α-amylase (PPA) binds to N-linked glycans of glycoproteins (Matsushita, H., Takenaka, M., and Ogawa, H. (2002) J. Biol Chem., 277, 4680–4686). Immunostaining revealed that PPA is located at the brush-border membrane (BBM) of enterocytes in the duodenum and that the binding is inhibited by mannan but not galactan, indicating that PPA binds carbohydrate-specifically to BBM. The ligands for PPA in BBM were identified as glycoprotein N-glycans that are significantly involved in the assimilation of glucose, including sucrase-isomaltase (SI) and Na$^+$/Glc cotransporter 1 (SGLT1). Binding of SI and SGLT1 in BBM to PPA was dose-dependent and inhibited by mannan. Using BBM vesicles, we found functional changes in PPA and its ligands in BBM due to the N-glycan-specific interaction. The starch-degrading activity of PPA and maltose-degrading activity of SI were enhanced to 240 and 175%, respectively, while Glc uptake by SGLT1 was markedly inhibited by PPA at high but physiologically possible concentrations, and the binding was attenuated by the addition of mannose-specific lectins, especially from Galanthus nivalis. Additionally, recombinant human pancreatic α-amylases expressed in yeast and purified by single-step affinity chromatography exhibited the same carbohydrate binding specificity as PPA in binding assays with sugar-biotinyl polymer probes. The results indicate that mammalian pancreatic α-amylases share a common carbohydrate binding activity and specifically bind to the intestinal BBM. Interaction with N-glycans in the BBM activated PPA and SI to produce much Glc on the one hand and to inhibit Glc absorption by enterocytes via SGLT1 in order to prevent a rapid increase in blood sugar on the other.

α-Amylase (EC 3.2.1.1) is an endoenzyme that typically cleaves the α1,4-Glc linkages of starch (1) and plays important roles in energy acquisition in bacteria, fungi, plants, and animals. Pancreatic α-amylase is synthesized in the pancreas and secreted into the pancreatic fluid with other pancreatic enzymes or zymogens and plays a role in the digestion of starch to produce maltose or larger oligosaccharides in the intestine, which are further processed by the exoenzymes located at the luminal brush-border membrane (BBM)[6] of enterocytes. The mammalian intestinal BBM is heavily glycosylated with N- and O-linked oligosaccharides that are produced by enterocytes and goblet cells to hold receptors of endogenous growth factors, hormones, and bacteria (2–6).

We previously showed that porcine pancreatic α-amylase (PPA) binds with the N-glycans of glycoproteins (7). This binding activity was not observed in α-amylases from *Bacillus subtilis*, plants, or human saliva. Following this discovery, we found that bovine and porcine pancreatic trypsins possess carbohy-

drate binding activities that are similar to PPA in their considerably high affinity to α-Man but different from PPA in their extremely high affinity to GalNAc/Gal (8). Although these pancreatic enzymes have been known since the first half of the 18th century, their carbohydrate binding activities had never been reported before. This raises the following questions. If these pancreatic enzymes do bind carbohydrates, what are the biological ligands and biological functions of the carbohydrate binding of these enzymes? Do the pancreatic enzymes of other animals, especially humans, bind to carbohydrates? The amino acid sequences of porcine and human pancreatic α-amylases have 86% identity and high similarity in their three-dimensional structures, including catalytic domains and subsites (9).

In this study, the glycoprotein ligands for pancreatic α-amylase in enterocytes were sought, and the biological effects of the interaction on Glc assimilation were studied. Furthermore, recombinant human pancreatic α-amylase (recHPA) was prepared to compare its carbohydrate binding activity with that of PPA. This is the first report that identifies the biological ligands for α-amylase with the exception of substrate starch and reveals novel functional changes occurring in BBM due to carbohydrate-specific interactions of this long-known enzyme. This study will open new windows into the modulatory role of cell surface glycans for metabolic homeostasis.

EXPERIMENTAL PROCEDURES

Materials

PPA was purchased from Elastin Products Co., Inc. (Owensville, MO). Horseradish peroxidase (HRP)-conjugated rabbit anti-α-amylase antibody (ab34578) and rabbit anti-Na$^+$/Glc cotransporter 1 (SGLT1) antibody (ab14686) were purchased from Abcam (Cambridge, MA). Rabbit anti-sucrase-isomaltase (SI) antibody (number 190) was purchased from Santa Cruz Biotechnology, Inc. (Santa Cruz, CA). Rabbit anti-human pancreatic α-amylase antibody (A36) was purchased from Biomeda Corp. (Foster City, CA). HRP-conjugated goat anti-rabbit IgG was obtained from Kirkegaard & Perry Laboratories, Inc. (Gaithersburg, MD). Sugar-biotinyl polymer (BP) probes were purchased from GlycoTech Co. (Gaithersburg, MD). HRP-conjugated avidin-biotin complex (ABC-HRP) was purchased from Sigma. Phlorizin was provided by Toronto Research Chemicals Inc. D-[^{14}C(U)]Glc (3.7 MBq/ml (100 μCi/ml)) was purchased from Moravek Biochemicals (Brea, CA). Bacto-yeast nitrogen base without amino acids was from BD Biosciences. Lectins from *Galanthus nivalis* (GNA), peanut lectin, *Maackia amurensis* mitogen, and *Phaseolus vulgaris* lectin type L were purchased from Seikagaku Corp. (Tokyo, Japan). *Canavalia ensiformis* concanavalin A (ConA) was purified in our laboratory using a maltamyl-Sepharose column (10). Biotin-labeling of lectins and PPA was done in the presence of protecting sugar for each protein as described previously (11). α-Mannan from *Saccharomyces cerevisiae* and β-galactan from gum arabic were purchased from Sigma-Aldrich. Other sugars and chemical reagents were purchased from Wako Pure Chemicals Inc. (Osaka, Japan) or Nacalai Tesque (Kyoto, Japan).

Immunohistochemistry

PPA was dissolved at 10 μM (0.56 mg/ml) in either 20 mM phosphate-buffered saline (PBS, pH 7.2) or PBS (pH 7.2) containing α-mannan or β-galactan, concentrations that correspond to a 0.1 M concentration of the constituent sugar, D-Man, or D-Gal residue, respectively, and incubated overnight at 4 °C. Porcine duodenum from fasting animals was washed with cold 20 mM PBS (pH 7.2) and cut into 1-cm cross-sections. The fresh duodenum sections were soaked in 20 mM PBS (pH 7.2) or PBS (pH 7.2) containing 10 μM PPA in the absence or presence of mannan or galactan and incubated at 4 °C for 0–30 min with gentle agitation. After incubation, the tissues were fixed in formalin, and paraffin-embedded sections were prepared. For detection of PPA, the sections were deparaffinized and rehydrated, and endogenous peroxidase was inactivated by treatment with 3% H$_2$O$_2$ for 6 min. The sections were washed with 10 mM Tris-HCl-buffered saline, pH 7.2 (TBS), and blocked with 2% skim milk in TBS for 30 min, incubated with HRP-conjugated rabbit polyclonal anti-α-amylase antibodies (diluted to 1:150) overnight at 4 °C, and then washed with 10 mM TBS. The untreated sections were stained with rabbit anti-SGLT1 antibody (diluted to 1:50) or rabbit anti-SI antibody (diluted to 1:50) as described previously (11). After washing with 10 mM TBS three times, the sections were reacted with HRP-conjugated goat anti-rabbit IgGs (diluted to 1:200 with 10 mM TBS) at room temperature for 1 h and then washed with 10 mM TBS. The sections were developed with 3,3'-diaminobenzidine tetrahydrochloride (DAB) and H$_2$O$_2$ in 10 mM TBS containing 0.1% Tween 20 for 7 min and then counterstained with hematoxylin (11). Bright field images were taken using an FSX100 microscope (Olympus Optical Co., Ltd., Tokyo, Japan).

Preparation of Brush Border Membrane Vesicles from Porcine Duodenum

Brush border membrane vesicles (BBMV) were isolated from duodenal mucosa of five pigs by the Ca^{2+} precipitation method as described previously (12). All steps were performed at 0–4 °C. The isolated membranes were suspended in the appropriate buffer for each assay. Purification of the BBMV fraction was confirmed by measuring the alkaline phosphatase (EC 3.1.3.1) activity, which is a marker of BBMV (13), in a microtiter plate using p-nitrophenyl phosphate as a substrate (14). The protein concentration was determined by BCA protein assays (Thermo Fisher Scientific Inc., Rockford, IL) using bovine serum albumin as a standard. BBMV was purified more than 18-fold from that in homogenate as measured by the alkaline phosphatase activity.

Affinity Chromatography of BBM Fraction on PPA-Sepharose Column

PPA-Sepharose was prepared by coupling 45 mg of salt-free PPA with formyl-Sepharose 6B (20 g) (7) in 25 ml of 5 mM CaCl$_2$, 0.15 M NaCl, and 10 mM HEPES-NaOH buffer (pH 8.0) containing 0.2 M methyl α-D-mannnopyranoside (Me α-Man), 0.1 M Me β-Gal, and 0.1 M Me α-D-Glc, as protecting sugars, and 240 mg of NaCNBH$_3$ at 4 °C for 2 days. Excess formyl groups were blocked with 40 ml of 1 M Tris-HCl (pH 7.2) containing 120 mg of NaCNBH$_3$ at 4 °C for 1 day. About 1.5 mg of PPA/ml

of gel was calculated to be immobilized from the difference in absorbance of the supernatants before and after coupling at 280 nm. The BBMV was used immediately after preparation and was solubilized by adding Triton X-100 to 1% (v/v), followed by incubation at 4 °C overnight and then dilution to one-tenth concentration with 10 mM TBS, containing 5 mM CaCl$_2$ (TBS-Ca). All three chromatography steps were performed at 0–4 °C. The eluted proteins were monitored by BCA protein assays.

Chromatography 1 (Sepharose 6B Precolumn)—Sepharose 6B column (20 ml, 1.5 × 12.5 cm) was equilibrated with TBS-Ca containing 0.1% Triton X-100. The solubilized BBM (20 mg as protein/10 ml in equilibration buffer) was applied and washed with the equilibration buffer. The bound proteins were eluted with Me α-Man in equilibration buffer and finally with 0.1 M borate buffer (pH 8.0) containing 0.1% Triton X-100.

Chromatography 2 (First Affinity Chromatography—The pooled pass-through fractions obtained in Step 1 were mixed with PPA-Sepharose 6B that had been (20 ml) equilibrated with TBS-Ca and incubated in a sealed tube with gentle rotation at 4 °C for 1 day. The mixture was packed into a glass column (1.5 × 12.5 cm) and washed with TBS-Ca. After various elution conditions were examined, the following procedure was used. The bound proteins were eluted with 0.2 M Me α-Man in 10 mM TBS, pH 7.2, containing 25 mM EGTA and 0.1% Triton X-100, and finally with 0.1 M borate buffer, pH 8.0, containing 25 mM EGTA and 0.1% Triton X-100. Steps 1 and 2 were carried out twice, and the two E1 fractions were combined for the next step.

Chromatography 3 (Second Affinity Chromatography)—The two pooled fractions (E1) eluted from the first PPA-Sepharose column were dialyzed against TBS-Ca to remove Me α-Man and concentrated using an Amicon ultrafiltration apparatus (YM10 membrane, Millipore, Billerica, MA) to 1.6 ml. The concentrated sample was mixed with 2 ml of PPA-Sepharose 6B, and incubation, washing, and elution were performed as described in step 2. The pooled eluted fractions (E2) from the second PPA-Sepharose elution were concentrated using a Microcon® YM-3 (Millipore).

Identification of Protein by LC/MS/MS Analysis

The solubilized BBM proteins that bound to and were eluted from the first and second PPA-Sepharose column were separated by SDS-PAGE. The SYPRO Ruby (Invitrogen)-stained protein bands were cut out of the gel and dried. The protein in each gel band was carboxymethylated and incubated with 20 µg/ml trypsin in 25 mM ammonium bicarbonate. The digest extracted from the gel was subjected to LC/MS/MS using a liquid chromatograph (Paradigm MS4 HPLC system, Michrom BioResources, Auburn, CA) connected to an ion trap-type mass spectrometer (LTQ; Thermo Fisher Scientific, Waltham, MA) equipped with a nanoelectrospray ion source (AMR, Tokyo, Japan). The mobile phase was 0.1% formic acid containing 2% acetonitrile (buffer A) and 0.1% formic acid containing 90% acetonitrile (buffer B). The peptides were separated at a flow rate of 300 nl/min by using a reversed-phase column (L-column Micro; 150 × 0.075 mm, 3 µm; Chemicals Evaluation and Research Institute, Tokyo, Japan) with a 2–65% gradient of buffer B in 50 min. The conditions for MS/MS were electrospray voltage of 2.0 kV in positive ion mode, capillary temper-

ature of 200 °C, tube lens offset of 140 V, and collision energy of 35% for MS/MS. The spectra data obtained by MS/MS were subjected to database search analysis using the Turbo-SEQUEST algorithm (BioWorks 3.1; Thermo Fisher Scientific) with the NCBI nr database (21-02-09). The static modification of carboxymethylation (58.0 u) at Cys was used as the modified parameters for database search analysis. The SEQUEST criterion, known as peptide probability, was set to 0.001 for the protein identifications.

Reactivity of PPA-binding Proteins with Biotin-lectins

The solubilized BBM (10 µg) and the bound fraction eluted from the PPA column were subjected to SDS-PAGE on a 7.5% polyacrylamide gel under reducing conditions and electroblotted onto a PVDF membrane (15). The membrane was blocked with 3% BSA in 10 mM TBS, cut into lanes, and probed with each biotin-lectin or biotin-PPA (10 µg/ml in 10 mM TBS) for 1 h at room temperature. In the case of peanut lectin, the blotted membrane was probed with biotin-peanut lectin before and after treatment with 0.025 M H$_2$SO$_4$ at 80 °C for 1 h for desialylation. The bound lectins or PPA were detected with ABC-HRP (diluted 1:500 in 10 mM TBS) for 1 h at room temperature and subsequently with DAB (0.2 mg/ml) and 0.006% H$_2$O$_2$ in 0.1 M citrate-phosphate buffer, pH 5.5.

ELISA Studies of Binding between PPA and SI or SGLT1

Various concentrations of PPA (1–50 µg/ml, 100 µl) were immobilized in wells of a microtiter plate (Immulon 1B, Dynex) in TBS-Ca overnight at 4 °C. After the wells were washed with TBS-Ca and blocked with 3% BSA in TBS-Ca, the solubilized BBM (0.1 mg/ml, 100 µl) was added and incubated for 2 h at room temperature. After the wells were washed three times with TBS-Ca and blocked with 3% BSA in TBS-Ca for 2 h at room temperature, the antibodies against SI (diluted 1:1,000) or SGLT1 (diluted 1:4,000) were added and incubated for 2 h at room temperature. After washing with TBS-Ca, the bound IgG was detected with HRP-conjugated anti-rabbit IgG (diluted 1:1,000) for 1 h at room temperature, developed with o-phenylenediamine (0.4 mg/ml) and 0.008% H$_2$O$_2$ in 0.1 M citrate-phosphate buffer, pH 5.0, and measured at 490 nm. For the inhibition studies, various concentrations of mannan or galactan in TBS-Ca (0.5–5 mg/ml, 50 µl) were added to the immobilized PPA in the wells and preincubated overnight at 4 °C, and then solubilized BBM (0.2 mg/ml, 50 µl) was added, and ELISA was performed as described above.

Binding to Sugar-BP Probes

Binding to sugar-BP probes was measured by ELISA. PPA and recHPA were immobilized in wells of a microtiter plate (Immulon 1B, Dynex) at concentrations of ~20 µg/100 µl in TBS-Ca overnight at 4 °C. All other procedures were performed at room temperature using the same buffer according to the procedure described previously (7).

Measurement of Starch-degrading Activity

The α-amylase activity was measured according to the method of Bernfeld (7) on a small scale. To evaluate the effect of Triton X-100, 10 nM PPA (0.56 µg/ml, 25 µl) in 20 mM PBS, pH

6.9, was preincubated with various concentrations of Triton X-100 (1×10^{-5} to 10^{-1}% (v/v), 25 μl), glycoprotein (thyroglobulin, 500 nM, 25 μl), or BBMV (0.56–167 μg/ml, 25 μl) at 37 °C for 15 min, and 0.1 ml of 1% starch in 20 mM phosphate buffer, pH 6.9, was added. The mixture was reacted at 37 °C for 30 min. To stop the reaction, 0.1 ml of 3,5-dinitrosalicylic acid reagent was added, and the mixture was heated at 98 °C for 5 min to develop the color. The reaction mixture was cooled on ice. Aliquots (50 μl) of the reaction mixture were diluted with 200 μl of water in a 96-well microtiter plate and measured at 540 nm. Maltose was used as a standard for reducing sugar. In order to correct the interference by the endogenous reducing sugar, PPA and BBMV that had been heat-treated at 98 °C for 20 min were used as blanks.

To suppress the incorporation of Glc, the final degradation product of starch, into the vesicles by the action of SGLT1, the SGLT1 inhibitor 0.5 mM phlorizin was added to the BBMV suspension. Prior to this assay, phlorizin was confirmed to have no effect on the activities of purified PPA and endogenous PPA in BBMV (data not shown).

Because Glc is a product of the degradation of disaccharides by the action of SI and is normally taken up into the vesicles by the action of SGLT1, we inhibited Glc transport into BBMV by adding 0.5 mM phlorizin, an SGLT1 inhibitor, to the reaction mixture. Phlorizin was confirmed not to affect the sucrose or maltose degradation activity on BBMV under these conditions (data not shown).

Measurement of SI Activity

SI activities in BBMV were measured as described previously (16), using maltose or sucrose as the substrate. After examining various concentrations of BBMV and reaction times, BBMV was used at protein concentrations of 0.2 and 1.0 mg/ml, and the following reaction times were used. Various concentrations of PPA or ConA (25 μl) were added to BBMV (12.5 μl) with 1 mM phlorizin, and maltose or sucrose (each 0.112 mM, 12.5 μl) was added. After 30 min for maltose or 60 min for sucrose, the ice-cold stop solution in Tris-HCl was added. The Glc generated was measured enzymatically using the Wako Glc CII test (Wako Pure Chemicals, Osaka, Japan).

Because Glc is a product of the degradation of disaccharides by the action of SI and is normally taken up into the vesicles by the action of SGLT1, we inhibited Glc transport into BBMV by adding 0.5 mM phlorizin, an SGLT1 inhibitor, to the reaction mixture. Phlorizin was confirmed not to affect the sucrose or maltose degradation activity on BBMV under these conditions (data not shown).

Measurement of SGLT1 Activity Using Porcine Duodenum BBMV

The uptake of D-[^{14}C(U)]Glc was measured by a rapid filtration technique as described previously (17). Usually, BBMV were suspended in 10 mM HEPES-Tris buffer, pH 7.5, containing 100 mM mannitol and preincubated for 2 min at room temperature. The Glc solution (20 μl) consisting of 0.2 mM D-[^{14}C(U)]Glc (final 0.1 mM), 10 mM HEPES-Tris, pH 7.5, 100 mM mannitol, and 200 mM NaCl or 200 mM KCl was added to 20 μl of BBMV suspension at room temperature to initiate the

reaction. After 5 s, the reaction was terminated by adding 1 ml of an ice-cold stop solution containing 150 mM NaCl, 20 mM HEPES-Tris, pH 7.5, and 0.1 mM phlorizin. The mixture was immediately poured onto Millipore filters (HAWP, 0.45 μm, 2.5-cm diameter), and the filters were washed with 5 ml of the ice-cold stop solution. The D-[^{14}C(U)]Glc radioactivity that was trapped in membrane vesicles was measured by liquid scintillation counting using an ACS II scintillation cocktail (Amersham Biosciences).

To measure the effects of PPA and lectins, double concentrations of the BBMV suspension and Glc solution (10 μl each) were used, and 10 μl of either PPA or lectin in suspension buffer was added just before adding the Glc solution.

Expression and Purification of recHPA

The plasmid YEp-HPASIG, designed to express a pre-HPA gene with a GAL 10 promoter in yeast, was constructed from the plasmid pAMPA2 (18). Amylose-Sepharose was prepared in our laboratory. Sepharose 6B was activated with divinyl sulfone (Pharmacia P-L Biochemicals, Inc., Milwaukee, WI) according to the method of Fornstedt and Porath (19) and reacted with amylose (Nacalai Tesque) in 20 ml of 0.5 M carbonate buffer (pH 10) at room temperature for 1 day. Excess divinyl sulfone groups were blocked with 20 ml of 0.5 M bicarbonate buffer (pH 8.5) containing 400 μl of 2-mercaptoethanol at room temperature for 2 h, and the gel was washed extensively with water.

S. cerevisiae (W303-1A), which had been transformed with YEp-HPASIG or a mock plasmid, was selected on the SD−Leu medium described previously (1). Each selected yeast was inoculated into 1.5 liters of synthetic medium, SGal-Leu (0.67% yeast nitrogen base without amino acids, 5% Gal, 0.5% sucrose, and 1.3 g/liter amino acid mixture) supplemented with one-tenth volume of 1 M phosphate buffer, pH 7.5, and cultured at 30 °C with shaking at 180 rpm for 3 days. Then the culture medium was collected and centrifuged at $4,025 \times g$ for 10 min to remove yeast. All subsequent purification procedures were performed at 4 °C. The supernatant was concentrated to 80 ml using an Amicon ultrafiltration cell with a membrane with a cut-off size of 10 kDa (YM-10, Millipore). The concentrate was loaded onto an amylose-Sepharose column (1.3×8 cm) pre-equilibrated with TBS-Ca. After washing the column, bound recHPA was eluted with 0.2 M maltose in 10 mM TBS and monitored by absorbance at 280 nm. The peak fractions were pooled, dialyzed, and concentrated against 10 mM TBS using an ultrafiltration cell.

Reactivities of Antibodies to recHPA or PPA on Membrane

The immunoreactivity of recHPA or PPA was studied after SDS-PAGE using 9.5% polyacrylamide gel and electroblotting onto a PVDF membrane as described previously (15). The blotted membranes were blocked with 3% BSA in 10 mM TBS and cut by lane. One lane was reacted with 2 μg/ml rabbit anti-human pancreatic α-amylase antibody (Biomeda A36) in 10 mM TBS for 2 h at room temperature and washed with 10 mM TBS. The bound IgG was detected with 2 μg/ml HRP-conjugated anti-rabbit IgG for 1 h at room temperature and visual-
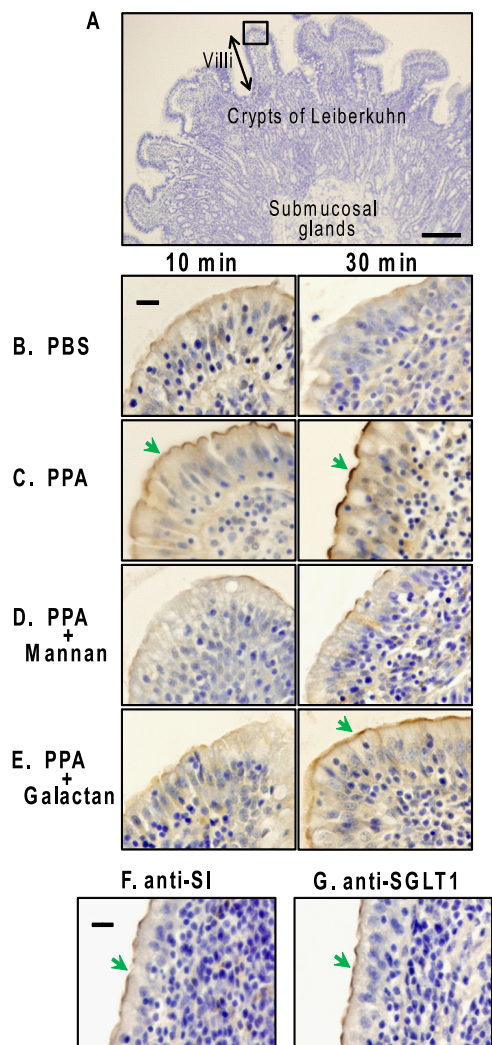
FIGURE 1. **Immunohistochemical staining of PPA in porcine duodenum.** Porcine duodenum sections (*A*) from fasted animals were incubated with 20 mM PBS (*B*) or various PPA solutions (*C–E*) containing 1 mM phenylmethylsulfonyl fluoride at 4 °C for 10 and 30 min and then fixed and paraffin-embedded as described under "Experimental Procedures." The paraffin sections were immunostained with rabbit anti-α-amylase IgGs-HRP (*B–E*). The *color* was developed with DAB/H_2O_2 and then counterstained with hematoxylin. *Green arrows* indicate positive staining on the apical surface (*A*) the luminal side of the duodenum. The tip of a villus surrounded by a *square* in *A* is shown in *B–G*. Duodenum sections were incubated in 20 mM PBS (*B*), 10 μM PPA (*C*), 10 μM PPA containing mannans (*D*), or galactans (*E*). Untreated porcine duodenum sections were detected with rabbit anti-SI IgGs-HRP (*F*) and SGLT1 (*G*). *Scale bar* in *A*, 100 μm; *scale bars* in *B* and *F*, 20 μm. Similar experiments were repeated three times.

ized with DAB/H_2O_2, as described for the reactivity with biotin-lectins.

RESULTS

Binding of PPA to Porcine Duodenum—Because PPA is synthesized in acinar cells and secreted into the pancreatic fluid, we used duodenum sections from fasted animals to avoid commingling antecedents of endogenous PPA and its degradation products in the intestine. To detect fresh PPA in the duodenum by the antibody, exogenous PPA was added to the fresh duodenum sections. Fig. 1*A* shows the microscopic appearance of the luminal side of the duodenum. Comparison of Fig. 1*B* with Fig. 1*C* shows that the added PPA localized at the apical surface of

villi (indicated by a *green arrow*) and had increased markedly after 30 min of incubation compared with that at 10 min. As shown in Fig. 1*D*, mannan inhibited the binding of PPA to the apical surface almost completely, whereas galactan inhibited it to a lesser extent (Fig. 1*E*), indicating that PPA bound to the BBM of enterocytes via carbohydrate-specific interaction with the BBM components. Bound PPA was little incorporated into the enterocytes at 4 °C. To confirm that PPA bound to the BBM in the duodenum, the immunolocalizations of the marker enzymes for BBM of enterocytes, SI and SGLT1 (20), were compared. As shown in Fig. 1, *F* and *G*, SI and SGLT1 were expressed at the apical surface (indicated by a *green arrow*), which coincided with the localization of PPA. The results indicated that PPA introduced in duodenum bound to the apical surface via *N*-glycan ligands in BBM.

Identification of PPA Ligands in BBM—The ligands that link α-amylase to the BBM have never been identified. Therefore, we purified and identified the PPA-binding ligands in the BBM by affinity chromatography using a PPA column and then examined whether they possess *N*-glycans that PPA can bind to. The binding and elution were performed in 0.1% Triton X-100 because it achieved high solubilization efficiency among the detergents examined (data not shown) without damaging the carbohydrate binding activity of PPA (Fig. 6*A*). Because Triton X-100 absorbed the ultraviolet light and interfered with the protein monitoring by absorbance at 280 nm, protein monitoring in affinity chromatography was performed by a BCA protein assay (Fig. 2).

Although a peak was detected during elution with borate buffer from a Sepharose precolumn on the BCA assay (Fig. 2*A*), no band stained with SYPRO Ruby on SDS-PAGE of the fraction. The pass-through fraction (*P*) was applied to the PPA column. As shown in Fig. 2*B*, the bound proteins were specifically eluted with Me α-Man in a single protein peak (peak E1). Among the sugars tested, only Me α-Man succeeded in eluting the bound proteins from a PPA-immobilized column, revealing that PPA bound best to α-Man-BP among the sugar-BP probes at neutral pH (7). No more protein was eluted by a subsequent elution with borate buffer. Fractions of peak E1 were pooled and again applied to a PPA column to sort the high affinity ligands because multiple bands were present in peak E1 on SDS-PAGE (Fig. 3, *lane E1*). As summarized in Table 1, the amount of PPA-binding protein was reduced by the second affinity chromatography, but peaks E1 and E2 gave similar electrophoretic patterns, except that the 60–65 kDa band (indicated by an *asterisk*), which was identified as human keratin contamination acquired during the second chromatography step, increased in E2 (Fig. 3).

The major bands of *lanes E1* and *E2* were cut out of the gel and digested with trypsin, and proteins were identified by LC-MS/MS and a database search. No proteins were identified from the SYPRO Ruby-positive top edge of the gel. The proteins (also indicated in Fig. 3, *right*) were identified as follows: band I (202 kDa), SGLTs (intact molecular mass 48–73 kDa), which have been reported to form tetramers in BBM (21), and SI (69 kDa) in E1 (fraction E2 contained mainly trypsin, which had been used for protein identification by mass analysis, and serum albumin and pancreastatin were detected with low scores (<20));
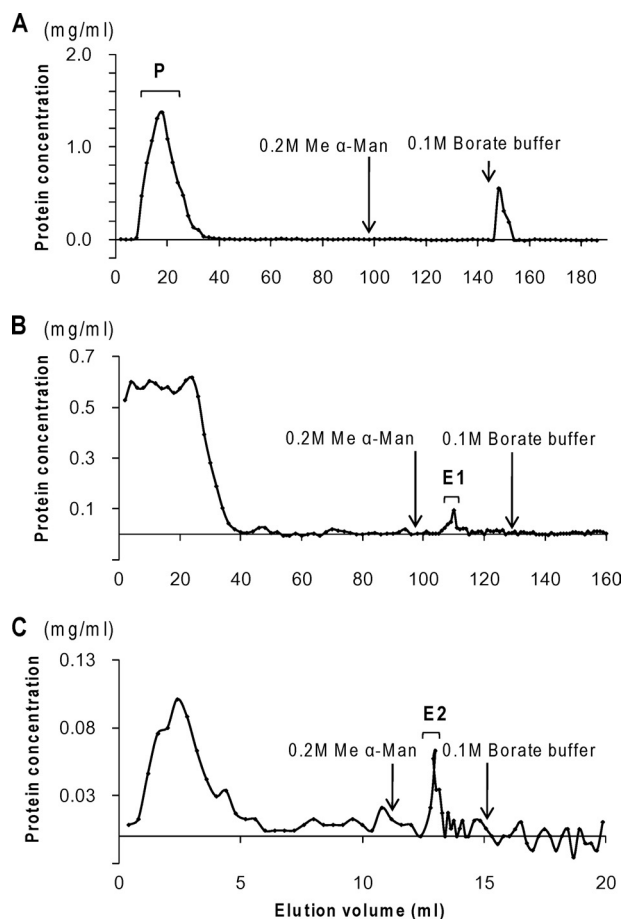
FIGURE 2. **Affinity chromatography of BBM components on PPA-Sepharose.** *A,* the solubilized BBM was applied to a Sepharose 6B column. After washing with TBS-Ca containing 0.1% Triton X-100, the pass-through fractions (*P*) of BBM components were collected. *B,* the pass-through fractions were applied to a PPA-Sepharose column, and the proteins bound to PPA-Sepharose were eluted with 0.2 M Me α-Man in 10 mM TBS containing 25 mM EGTA and 0.1% Triton X-100 as E1. *C,* rechromatography of fraction E1 on a PPA-Sepharose column. The eluted proteins (E2) were detected by BCA assay. Similar experiments were repeated four times.

FIGURE 3. **Identification of PPA-binding proteins in BBM.** The pass-through fractions from a Sepharose 6B column (*lane P*), the Me α-Man-eluted fractions from the first PPA column (*lane E1*), and those from the second PPA column (*lane E2*) were pooled separately, treated with 1% SDS and 2.5% 2-mercaptoethanol at 100 °C for 5 min, and analyzed by SDS-PAGE using 7.5% polyacrylamide gel (1.5 μg/lane), together with the solubilized BBM (*lane BBM*). The proteins were detected with SYPRO Ruby protein gel stain. The values on the *left* indicate the migration positions of the molecular mass markers. The proteins of *lane E1* and *E2* were identified by LC-MS/MS after trypsin treatment of each gel band, as described under "Experimental Procedures." On the *right*, the proteins identified from both E1 and E2 are shown, and those identified from only E1 but not from E2 are shown in *parentheses*. *, contaminating human keratin bands were detected in E2. *VLA-2,* integrin very late antigen-2; *DPP-IV,* dipeptidylpeptidase IV; *ACE 2,* angiotensin-converting enzyme 2.

TABLE 1

Purification of ligands for PPA from solubilized BBM

		Yield	
Chromatography step	Protein	Stepwise yield	Total (BBM = 100%)
	mg	*%*	*%*
BBM extract	40		100
Sepharose 6B precolumn	25.2	63.0	63.0
First PPA-Sepharose 6B	0.235	0.93	0.59
Second PPA-Sepharose 6B	0.008	3.42	0.02

band II (144–156 kDa), aminopeptidase N (109 kDa), glutamyl aminopeptidase (109 kDa), aminopeptidase (33 kDa), and integrin very late antigen-2 (21 kDa) in both E1 and E2 and enterokinase (115 kDa) in E1; band III (110–122 kDa), dipeptidylpeptidase IV (88 kDa), integrin subunit β-1 (88 kDa), and angiotensin-converting enzyme 2 (peptidyl-dipeptidase A, 92 kDa) in both E1 and E2 and SGLT in E1; band IV (99 kDa), aminopeptidase and aminopeptidase N in both E1 and E2; band V (78 kDa), transferrin (77 kDa) in both E1 and E2 and transferrin receptor (86 kDa) and SGLT1 (67 kDa) in E1; band VI (50–57 kDa), amine oxidase B (58–60 kDa), Na$^+$/K$^+$-ATPase β1-subunit (35 kDa), and enterokinase in both E1 and E2 and SGLT1 in E1; and band VII (46 kDa), epoxide hydrolase (52 kDa) and aminopeptidase N in both E1 and E2 and cation-dependent mannose 6-phosphate receptor (46 kDa; mannose 6-phosphate receptor, 46 kDa) in E1. The gaps between the molecular masses reported for the identified proteins (shown in *parentheses*) and those observed on SDS-PAGE (Fig. 3) would be attributable to the post-translational modification, including glycosylation and/or multimerization.
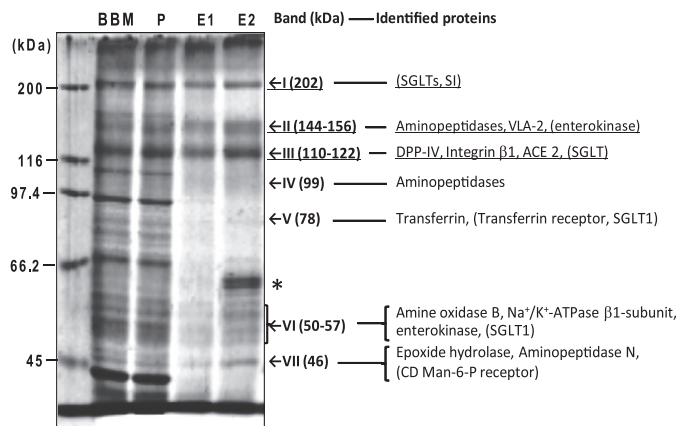
The ligands for PPA can be classified into three functional groups: group 1, which includes proteins that are stably present at the plasma membrane and play a role in digestion and absorption of Glc and includes SGLTs (22) (bands I, III, V, and VI) and SI (EC. 3.2.1.10/48, band I) (23); group 2, which consists of proteins that have a role in digestion of proteinaceous materials (*i.e.* aminopeptidases (bands II, IV, and VII), such as aminopeptidase N (EC 3.4.11.2) (24) and glutamyl aminopeptidase (EC 3.4.11.7), dipeptidylpeptidase IV (EC 3.4.14.5) (band III) (25), enterokinase (EC 3.4.21.9) (bands II, VII) (26), and amine oxidase (EC 1.4.3.6)); and group 3, which consists of proteins that are known to recycle between the plasma membrane and organelles, although their biological functions are diverse and some of them overlap with the group II members (*i.e.* transferrin (27) and transferrin receptor (28, 29) (both band V), integrin subunits (30) (bands II, III), cation-dependent mannose 6-phosphate receptor (31) (band VII), angiotensin-converting enzyme 2 (EC 3.4.15.1) (band III) (32–34), Na$^+$/K$^+$-ATPase (EC 3.6.1.3) (band VI) (35), dipeptidylpeptidase IV (band III) (25, 36), and aminopeptidase N (bands II, IV, and VII) (37)).

Because bands I, II, and III were major bands in terms of protein amounts, as judged by the intensities of SYPRO Ruby staining, the major candidate ligands for PPA were considered
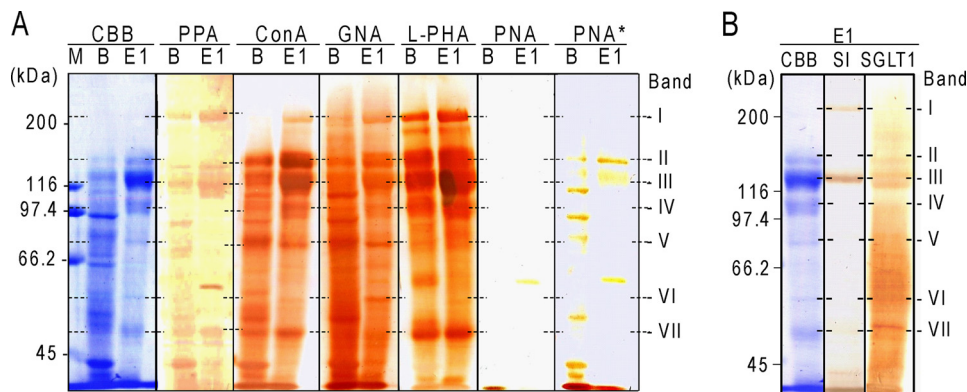
FIGURE 4. **Reactivity of PPA-bound proteins in BBM with biotin-PPA and various plant lectins.** *A*, proteins in the solubilized BBM (*B*) and peak fractions eluted from the first PPA column (*E1*) separated by SDS-PAGE, electroblotted onto a PVDF membrane, and then probed with biotin-PPA or various biotin-lectins before and after acid desialylation (indicated by an *asterisk*). *B*, similarly, fraction E1 was reacted on a membrane with anti-SI or anti-SGLT1 antibodies and detected with HRP-labeled anti-rabbit IgGs. The *color* was developed with DAB/H$_2$O$_2$ as described under "Experimental Procedures." The values on the *left* indicate the migration positions of the molecular mass markers (*lane M*). The values on the *right* indicate migration positions of bands I–VII. *CBB*, Coomassie Brilliant Blue. *L-PHA, Phaseolus vulgaris* lectin type L; *PNA*, peanut lectin.

to be the components of these bands: aminopeptidases, dipeptidylpeptidase IV, integrin subunits, angiotensin-converting enzyme 2, SGLT, SI, and enterokinase.

Reactivities of Lectin and PPA to PPA Ligands in BBM—The reactivities of the glycans of PPA ligands in BBM, which bound to and were eluted from the first PPA column (Fig. 2, *peak E1*), and the unfractionated BBM with various biotin-lectins and PPA were studied. Peak E1 was used because peak E2 did not contain enough protein for further assay (Table 1). As shown in Fig. 4, biotin-PPA bound clearly to the most protein bands of E1, indicating that the proteins directly bound to PPA in the column. The bands IV, V, and VI were scarcely stained by biotin-PPA, and the possibility remains that the proteins identified in these bands may be indirectly bound to PPA via some intermediary ligand proteins in BBM. Bands I–VII of peak E1 all bound to GNA and ConA, indicating the common presence of high Man-type *N*-glycans. Most bands except band VI bound to *P. vulgaris* lectin type L, suggesting the presence of complex-type tri- or tetraantennary *N*-glycans. Bands II and III bound to peanut lectin only after desialylation, indicating that the bands also contain *O*-linked sialylated core I glycans. All of the PPA ligands identified in Fig. 3 were glycosylated membrane proteins (28, 29, 33–35, 38–42); for example, SI consists of two subunits of sucrase and isomaltase. Both the subunits contain eight *N*-linked glycans, at least one of which is the high Man type (43). Human and porcine dipeptidylpeptidase IV possess nine and 11 *N*-glycosylation sites, respectively (25), and are *O*-glycosylated (43). The results indicate that the BBM ligands for PPA are all *N*-glycosylated glycoproteins possessing high Man-type and/or complex-type *N*-glycans and that some of them contain *O*-glycans of sialylated core 1 or other structures in addition to *N*-glycans. Comparison of the lectin binding patterns of *lane B* and *lane E1* indicates that there are many GNA-positive glycoproteins in BBM that were not present in E1, suggesting that the binding specificity of PPA is similar but not entirely identical to that of GNA.

Binding between PPA and Ligands in BBM by ELISA—Group 1 proteins in the candidate ligands for PPA, SI and SGLT1, were focused on because SI degrades the maltose that is produced when α-amylase breaks down starch (9), and SGLT1 transports
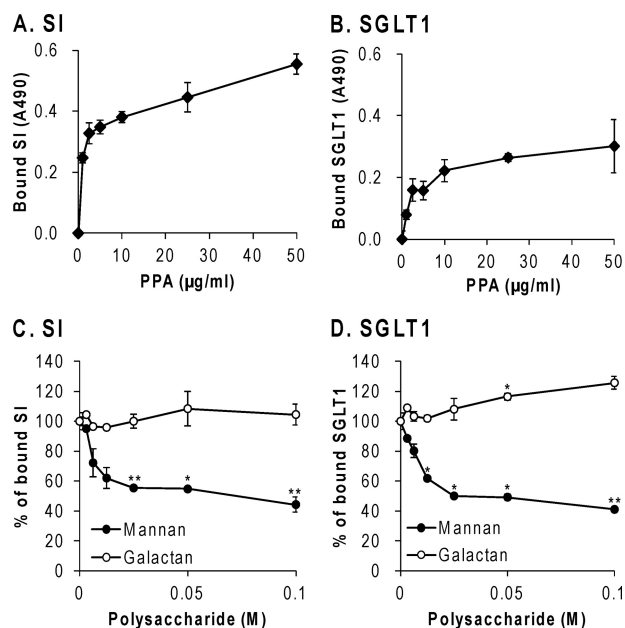

FIGURE 5. **Interaction studies between PPA and SI or SGLT1 in BBM by ELISA.** PPA was coated onto the wells of a microtiter plate and reacted with the solubilized BBM. The bound SI (*A* and *C*) and SGLT1 (*B* and *D*) were detected with each specific antibody and HRP-labeled secondary antibodies as described under "Experimental Procedures." *A* and *B*, concentration dependence of the binding on immobilized PPA. *C* and *D*, inhibition of the binding with polysaccharides. ●, mannan; ○, galactan. All experiments were carried out in duplicate and repeated three times. The data represent the means ± S.E. (*error bars*) (*n* = 3), and results for *C* and *D* were analyzed by Student's *t* test. *, $p < 0.01$; **, $p < 0.001$ compared with that in the absence of polysaccharides.

the Glc that is produced when SI breaks down maltose. The presence of SI and SGLT1 in fraction E1 was also demonstrated by immunoblotting, as shown in Fig. 4*B*. Positive staining with the antibodies was shown in band I and III for SI and bands III–VII for SGLT1, indicating the presence of these BBM glycoproteins, which agreed with the ligands identified in those bands by LC/MS/MS. In this study, solubilized BBM containing SI and SGLT1 was added to immobilized PPA on a microtiter plate, and the SI or SGLT1 bound to PPA was detected with the respective specific antibodies. As shown in Fig. 5, *A* and *B*, SI and SGLT1 concentration-dependently bound to PPA, sup-
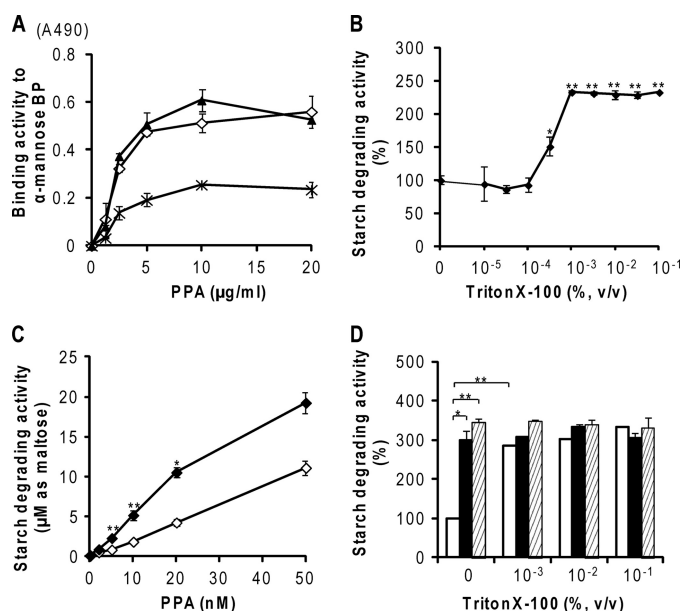
FIGURE 6. **Effects of Triton X-100 on carbohydrate binding and starch degradation by PPA.** *A*, effects of Triton X-100 on carbohydrate binding of PPA. PPA was coated onto the wells of a polystyrene plate and reacted with α-Man-BP probe in the absence (◇) or in the presence of 0.1% (▲) or 1.0% (✕) Triton X-100. The bound α-Man-BP probes were detected with ABC-HRP as described under "Experimental Procedures." All experiments were carried out in triplicate and repeated three times, and representative data from assays are shown, representing the means ± S.E. (*error bars*) (*n* = 3). *B–D*, effects of Triton X-100 on starch degradation of PPA. *B*, concentration dependence on Triton X-100. PPA was used at 10 nM. *C*, effects of 0.1% (v/v) Triton X-100 on activation induced by glycoprotein. Thyroglobulin (500 nM) was used as a glycoprotein ligand. PPA was used at 10 nM. ◇, PPA only; ◆, PPA + thyroglobulin. *D*, effects of 0–0.1% (v/v) Triton X-100 on activation induced by glycoprotein. □, PPA only; ■, PPA + thyroglobulin; ▨, PPA + heated thyroglobulin. All experiments were carried out in duplicate and repeated three times. The data represent the means ± S.E. (*n* = 3 for *B–D*) and were analyzed by Student's *t* test. *, *p* < 0.01; **, *p* < 0.001 compared with that in the absence of Triton X-100 (*B–D*) or that in the absence of thyroglobulin (*D*).

porting the hypothesis that SI and SGLT1 are PPA ligands in BBM. As shown in Fig. 5, *C* and *D*, mannan decreased the binding of PPA to SI and SGLT1 to the same extent, but galactan did not, which suggested that SI and SGLT1 in BBM interacted with PPA through the high Man-type *N*-glycans.

Effects of Triton X-100 on Carbohydrate Binding and Starch-degrading Activity of PPA—For the affinity chromatography and binding assays of PPA-binding proteins by ELISA, BBM was solubilized with 0.1% Triton X-100. As shown in Fig. 6*A*, the carbohydrate binding of PPA to α-mannose-BP in the presence of 0.1% Triton X-100 was at the same level as that in the absence of Triton X-100, whereas the binding of PPA was decreased to about half in the presence of 1% Triton X-100. Based on this result, the ligand isolation (Fig. 2) and binding study by ELISA (Fig. 5) were performed in 0.1% Triton X-100. However, because Triton X-100 exists as micelles at this concentration at 25 °C, it may interfere with the enzyme activities of PPA. Therefore, the effects of Triton X-100 were studied to choose the best experimental condition in which to evaluate the effect of binding of PPA to BBM.

As shown in Fig. 6, *B* and *C*, the presence of Triton X-100 at more than 10^{-3}% (v/v) unexpectedly more than doubled the starch-degrading activity of PPA. As shown in Fig. 6*C*, the enhancement of the starch-degrading activity of PPA in 0.1%

Triton X-100 was observed throughout the examined concentration range of PPA. However, the starch-degrading activity was proportional to the amount of PPA in the presence of 0.1% Triton X-100.

As shown in Fig. 6*D*, thyroglobulin added to PPA at a 50:1 molar excess enhanced the starch-degrading activity of PPA to 300% in the absence of Triton X-100. Thyroglobulin pretreated at 98 °C for 20 min to denature the protein moiety enhanced the activity of PPA to a similar extent as non-treated thyroglobulin in the absence of Triton X-100, indicating that PPA was enhanced by binding to the *N*-glycan moieties of thyroglobulin, which is heat-resistant. However, in the presence of Triton X-100 at more than 1×10^{-3}% (v/v), the enhancement of the starch-degrading activity of PPA by binding with thyroglobulin was hidden by the enhancing effect of Triton X-100. The results showed that the effect of ligand binding on the enzyme activity has to be studied in the absence of Triton X-100. However, Triton X-100 could not be removed by dialysis. We tried a specific resin to remove Triton X-100, but the target proteins were significantly decreased at the same time (data not shown). For these reasons, BBMV, instead of the purified E1 and E2 fractions that contain 0.1% Triton X-100, was used to study the effect of ligand binding on the starch-degrading activities of PPA.

Effect of BBMV on Starch Degradation by PPA—As shown in Fig. 7, BBMV were found to enhance the starch-degrading activity of PPA. When BBMV was added at 30-, 100-, and 300-fold excess by weight to PPA, it enhanced the enzyme activity of PPA to 210, 240, and 290%, respectively (Fig. 7*A*). Because the BBMV preparation sometimes contained α-amylase activity that was endogenous to the animal and had been incorporated into BBM, the BBMV was inactivated by heat treatment before the experiment. As shown in Fig. 7*B*, the enzyme activity of PPA was increased to 210, 240, and 230% in the presence of 30-, 100-, and 300-fold amounts of heat-treated BBMV, respectively, indicating that the enhancement with BBMV is unchanged when taking the loss of BBMV-resident activity due to heat treatment into account. This indicates that the starch-degrading activity of PPA was markedly enhanced when it bound to the glycan moieties of BBMV because glycans are heat-resistant.

Effect of PPA on Sucrase and Isomaltase Activities of SI—SI catalyzes the hydrolysis of sucrose and about 80% of dietary maltose, whereas maltase-glucoamylase (EC 3.2.1.20/3) catalyzes the hydrolysis of the remaining maltose (44, 45). Maltose is produced when α-amylase breaks down starch (46). SI activities in BBMV were assayed using maltose or sucrose as the substrate. As shown in Fig. 8*A*, PPA was found to enhance the maltose hydrolytic activity of SI to about 175%, whereas ConA did not. The addition of PPA had no effect on the sucrose hydrolytic activity of SI, whereas ConA slightly reduced it (Fig. 8*B*). The other two lectins, mannose-specific GNA and sialic acid-specific *M. amurensis* mitogen, did not affect either activity of SI (data not shown).

Effect of PPA on Glc Transport by SGLT1—Glc transport experiments were performed to evaluate the effect of PPA on Glc uptake by enterocytes in the duodenum. Using isolated porcine duodenal BBMV, Glc uptake showed a Na⁺-dependent
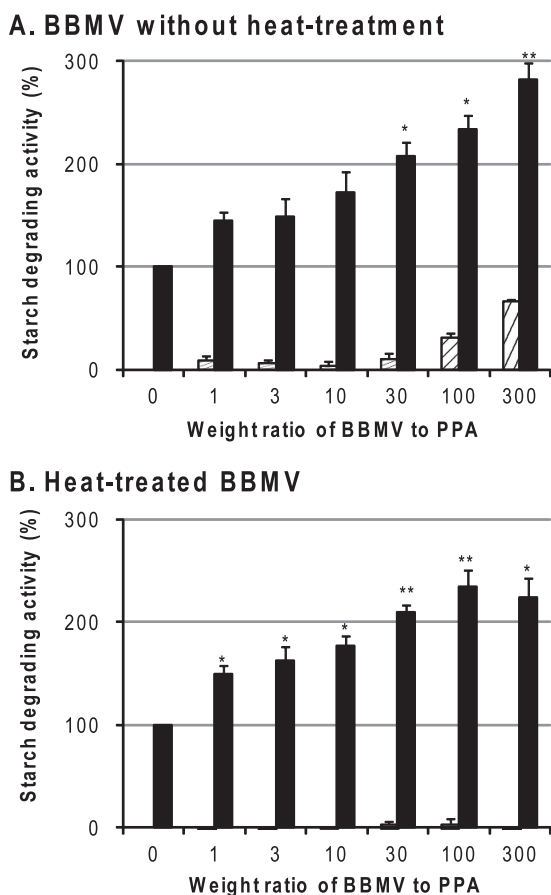
A. BBMV without heat-treatment

B. Heat-treated BBMV

FIGURE 7. **Effects of BBMV on starch degradation by PPA.** Various amounts of BBMV before (*A*) or after (*B*) heat treatment at 98 °C for 20 min to inactivate the BBM proteins were diluted to 0.56–167 μg/ml (25 μl) with the buffer containing 1 mM phlorizin, added to PPA (0.56 μg/ml (10 nM), 25 μl), and preincubated at 37 °C for 15 min. Then 0.1 ml of 1% soluble starch was added and reacted at 37 °C for 30 min, and the starch-degrading activity was measured by the concentration of reducing sugars, as described under "Experimental Procedures." The *ordinate axis* shows the PPA activity by taking that of standard PPA without BBMV as 100%. ▨, BBMV only; ■, PPA + BBMV. The experiment was carried out in duplicate and repeated three times. The data represent the means ± S.E. (*error bars*) (*n* = 3) and were analyzed by Student's *t* test after correcting the activity value for (PPA + BBMV) by subtracting the value for BBMV (*A*) or correcting the value for (PPA + heated BBMV) by subtracting the value for heated BBMV (*B*). *, $p < 0.05$; **, $p < 0.01$ compared with that in the absence of BBMV.

A. Maltose hydrolysis

B. Sucrose hydrolysis

FIGURE 8. **Effect of PPA on enzyme activities of SI.** The effect of Glc concentration in reaction mixtures was measured by using the Wako Glc CII test as described under "Experimental Procedures." ●, Glc concentration in the presence of PPA; ○, concentration of ConA. All experiments were carried out in triplicate and repeated two times. The data represent the means ± S.E. (*error bars*) (*n* = 3) and were analyzed by Student's *t* test. *, $p < 0.05$; **, $p < 0.01$ compared with that in the absence of PPA (●) or ConA (○).

overshoot (maximal at 60 s), indicating that an active transport process took place (Fig. 9*A*). In Fig. 9, *B* and *C*, the results at 5-s time points are presented after correction by subtracting the Glc uptake under a sodium-free condition, which was measured in the presence of 100 mM KCl. The presence of PPA at less than 5 μM did not significantly affect Glc uptake by BBMV (Fig. 9*B*). However, 10 μM PPA was found to decrease Glc uptake by about 65%. At the maximum concentration of PPA examined (20 μM), Glc uptake was inhibited by 90%. The half-maximal inhibitory concentration (IC_{50}) for the inhibitory action of PPA was calculated to be 8.1 μM using linear regression analysis.

Transport experiments in the presence of various lectins were performed to demonstrate whether carbohydrate-specific interaction between PPA and SGLT1 is responsible for the inhibition by PPA. As shown in Fig. 9*C*, the presence of each lectin alone in the assay system had little effect on Glc uptake. In
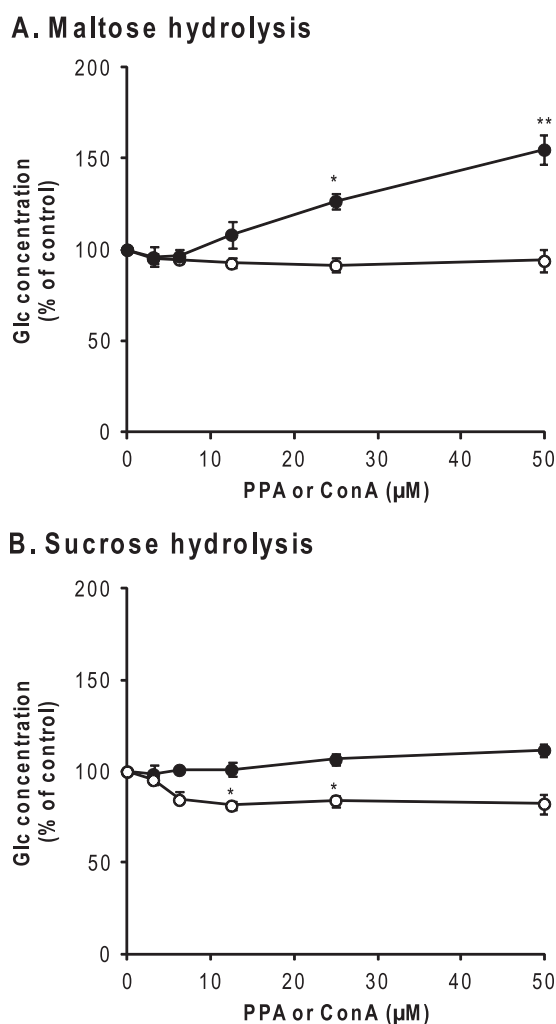
contrast, the copresence of a lectin and PPA neutralized the inhibition of Glc transport caused by PPA; GNA recovered the Glc uptake of BBMV from the inhibitory action by 10 μM PPA the most and ConA to a lesser extent, whereas *M. amurensis* mitogen had no effect on it (Fig. 9*C*). Because the carbohydrate content of PPA is less than 0.03% (w/w) (7), the neutralizing effect exhibited by the lectins is attributable to the binding of lectins to BBMV but not to PPA. In support of this, specific polysaccharides showed effects that are proportional to the binding activity with PPA; mannan attenuated the inhibitory action of PPA, whereas galactan did not (data not shown). The results indicate that PPA inhibited the Glc transport by SGLT1 through direct interaction with the *N*-glycans of SGLT1 or through indirect interaction with those of other BBM components.

Purification of recHPA—To examine whether recHPA has the same carbohydrate binding activity and BBM ligands as PPA, the recHPA was expressed in yeast. Fig. 10*A* shows that the yeast transfected with YEp51-HPA secreted proteins
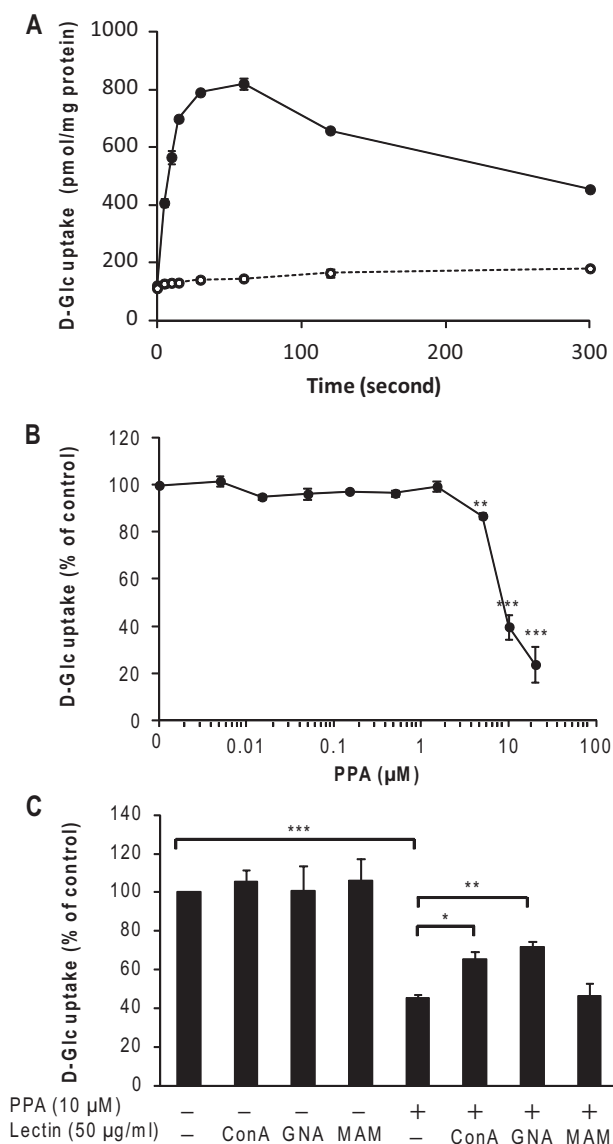
FIGURE 9. **Effect of PPA on SGLT1 activity.** *A*, time course of D-[^{14}C(U)]Glc uptake by porcine duodenum BBMV in 100 mM NaCl (●) or KCl (○) was measured during 5–300-s incubations. *B*, concentration dependence of D-Glc uptake on PPA. Glc uptake by BBMV was measured after incubation for 5 s as described under "Experimental Procedures." *C*, effects of PPA and lectins. PPA (20 μM, final 10 μM) and various lectins (100 μg/ml, final 50 μM) were added after preincubation of BBMV. All experiments were carried out in triplicate and repeated four times. The data represent the means ± S.E. (*error bars*) (*n* = 4 for *B* and *C*) and were analyzed by Student's *t* test. *, $p < 0.05$; **, $p < 0.01$; ***, $p < 0.001$ compared with that in the absence of PPA (*B* and *C*) and that in the absence of lectin (*C*). MAM, *Maackia amurensis* mitogen.

into the medium that were recognized by anti-HPA IgGs but that the mock transfectant did not, indicating that the positive bands are recHPA. The concentrated culture medium of the YEp51-HPA transformant was applied to an amylose-Sepharose column and eluted with 0.2 M maltose (Fig. 10*B*). The elution peak was separated into two fractions, peak 1 and peak 2. Peak 1 contained mainly 61- and 58-kDa proteins, whereas peak 2 contained 58- and 54-kDa proteins, and there were smear bands at around 80–130 kDa (Fig. 10*C*). The 61-, 58-, and 54-kDa proteins were considered to have two, one, and zero high Man-type *N*-glycans, respectively, whereas the 80–130 kDa smear band suggests that the recHPA possessed a gigantic

high Man-type glycan that is unique to yeast (see supplemental Figs. 1 and 2). The yield of total recHPA was calculated to be 0.84 mg/liter of medium from the absorbance at A_{280} based on $A^{1\%} = 21.0\ \text{cm}^{-1}$. The peak 2 fractions were further pooled separately as first, middle, and last eluted fractions because they differed in the extent of glycosylation. The last eluted fractions were almost devoid of gigantic α-mannosylation and used for further study as less glycosylated recHPA.

Interaction between recHPA and Sugar-BP Probes—Because the gigantic high Man glycans of recHPA interfered with the binding to the sugar-BP probes,[7] the less glycosylated recHPA was used for this study. As shown in Fig. 11*B*, recHPA bound best with α-mannose-BP among the probes examined and with α-mannose 6-phosphate-BP and α-GalNAc-BP to lesser extents. In contrast, the sugar-BP probes containing Lac, α-NeuAc, α-Gal, and LacNAc showed lower binding than the other probes. The results clearly indicate that recHPA exhibits essentially the same binding specificity toward sugar-BP probes as PPA does (Fig. 11*A*) (7).

DISCUSSION

Regulation of Glc Assimilation by N-Glycan-specific Interaction of α-Amylase in Duodenum—This study showed for the first time that α-amylases target carbohydrate-specific interactions to the duodenal BBM. We demonstrated that the biological significance of the carbohydrate-specific interaction between α-amylase and glycoligands in the intestine is to regulate Glc assimilation by using immunohistochemistry (Fig. 1), identification of glycoprotein ligands for PPA (Figs. 2–4), binding studies of glycoprotein ligands to PPA (Fig. 5), and alterations in the activities of starch degradation and Glc absorption in the interaction (Figs. 7–9). Additionally, we found that recHPA has the same carbohydrate binding activities as PPA (Fig. 11).

One discovery of this study and a new concept derived from the results are summarized schematically in Fig. 12. It was hitherto considered that α-amylase was devoid of a carbohydrate-specific interaction with *N*-glycans, and it had not been supposed to interact with BBM glycoproteins; therefore, α-amylase and SI are present but separate from each other and work without interaction to produce Glc. In the meantime, the Glc generated is intensively taken up by SGLT1 under the control of insulin, and that was the concept of intestinal starch degradation to date (Fig. 12*A*). In contrast, the findings in this study show that α-amylase binds to specific glycoprotein ligands in BBM of the duodenum and that both α-amylase and SI are allosterically activated to accelerate the starch degradation to produce Glc rapidly on the one hand (Fig. 12*B*, *left*), whereas uptake of Glc into enterocytes is suppressed by interaction between SGLT1 and a high concentration of PPA on the other hand to prevent a sudden increase in blood Glc. This is a novel regulation mechanism for blood sugar homeostasis (Fig. 12*B*, *right*). The gradual decrease of bound PPA by degradation, endocytosis, or dissociation will recover the Glc transport via SGLT1.

---

[7] K. Asanuma-Date, Y. Hirano, N. Le, H. Sakagami, and H. Ogawa, unpublished results.
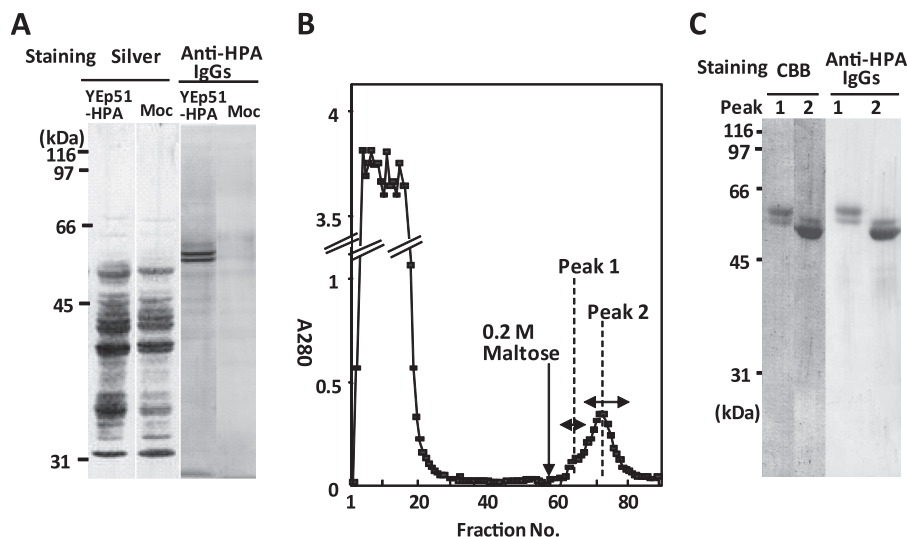
FIGURE 10. **Expression and purification of recHPA on amylose-Sepharose column.** *A*, HPA in yeast culture medium was concentrated by ultrafiltration 3 days after inoculation, and expression was analyzed by determining the reactivity with anti-HPA rabbit IgGs after SDS-PAGE, as described under "Experimental Procedures." *B*, elution profile of recHPA on an amylose column. recHPA was purified as described under "Experimental Procedures." *C*, fractions of peak 1 (fraction 63) and peak 2 (fraction 72) eluted from the amylose-Sepharose column were pooled, concentrated, and examined for recHPA by immunoreaction with anti-HPA IgGs. CBB, Coomassie Brilliant Blue.
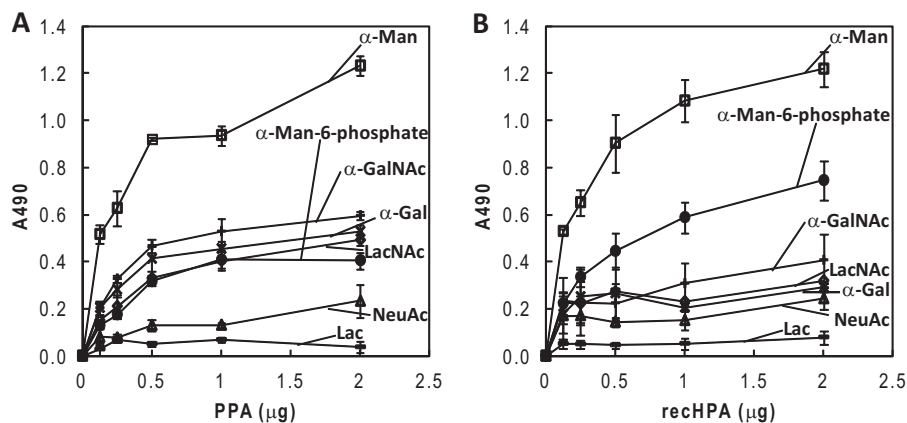

FIGURE 11. **Reactivities of PPA and recHPA with sugar-BP probes by ELISA.** PPA (*A*) and recHPA (*B*) were coated onto the wells of a polystyrene plate and reacted with various sugar-BP probes. The bound sugar-BP probes were detected by ELISA as described under "Experimental Procedures." □, α-Man-BP; ●, α-Man-6-phosphate-BP; +, α-GalNAc-BP; ×, α-Gal-BP; △, α-NeuAc-BP; —, Lac-BP; ◇, LacNAc-BP. All experiments were carried out in triplicate and repeated three times, and representative data from assays are shown, representing the means ± S.E. (*n* = 3).

Pancreatic α-amylase is present in the mammalian duodenum at a concentration that can exert the effects found in this study. The pancreatic fluid consists of various enzymes at concentrations, for example, of 4.2 mg/ml in healthy pigs and 5–16 mg/ml in cows (47), and the pancreatic fluid of the adult human contains much more protein than those of pigs and cows and is secreted in the amount of 1–3 liters/day. Because human pancreatic α-amylase comprises about 26.5% of the total proteins in the pancreatic fluid, the concentration of α-amylase must be higher than 1 mg/ml (48). Therefore, the concentrations of PPA used in Figs. 7–9 are physiologically possible concentrations in the duodenum of pigs, cows, and humans.

Types of N-Glycans of Glycoprotein Ligands for α-Amylase in Intestine—At neutral pH in the lumen of the intestine, PPA and recHPA interacted with α-Man residues much better than with β-Gal residues (Fig. 11), and PPA exhibited higher affinity to the glycoproteins having high Man-type glycans than to those having the complex type glycans.[7] The results of this study

showed that PPA interacted with *N*-glycans of BBM, especially the high Man types, due to the specific carbohydrate recognition as follows. The immunohistochemistry showed that the binding of PPA to the apical surface, which corresponds approximately to BBM, was completely inhibited by mannan and to a lesser extent by galactan (Fig. 1). When PPA ligands in duodenum BBM were identified by affinity chromatography, PPA-binding proteins were eluted only with Me α-Man, not with borate buffer or Me α-Gal (Fig. 2). PPA-binding proteins were demonstrated to have high-Man type and/or complex type *N*-glycans by lectin staining (Fig. 4). ELISA showed SI and SGLT1 bindings to PPA in BBM (Fig. 5, *A* and *B*), which were inhibited by mannan but not by galactan (Fig. 5, *C* and *D*). The starch degradation activity of PPA was remarkably enhanced in heat-treated BBMV, indicating that this enhancement is due to the interaction with glycans but not with protein moieties (Fig. 7). Inhibition of the D-Glc uptake via SGLT1 caused by PPA was most attenuated by

A. Traditional concept
＄Lack of carbohydrate-specific interaction of α-amylase＄
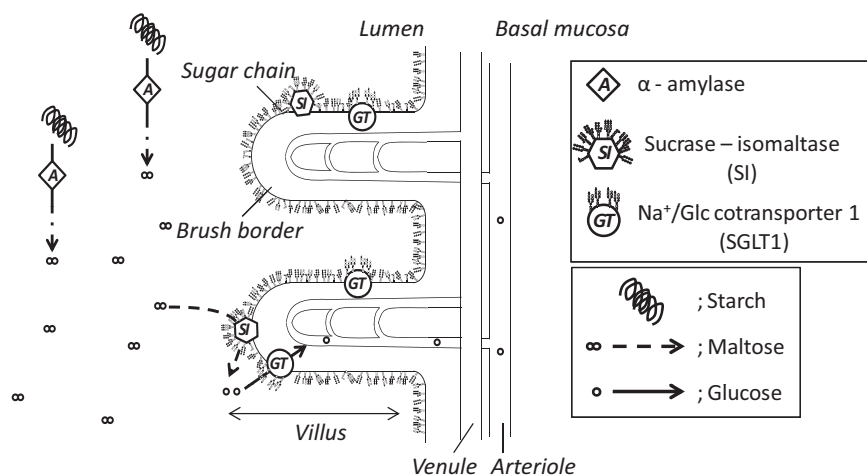
B. New concept presented in this study
＄Functioning carbohydrate-specific interaction of α-amylase＄

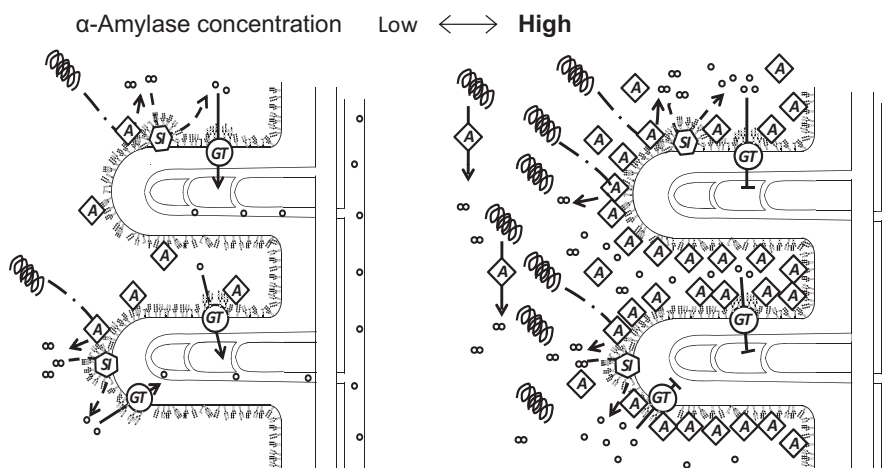α-Amylase concentration　　Low ⟷ **High**

FIGURE 12. **Schematic illustration of functional changes caused by *N*-glycan-specific interaction between α-amylase and BBM in duodenum.** *A*, if α-amylase is devoid of *N*-glycan-specific binding, it remains apart from BBM and SI. α-Amylase and SI separately catalyze starch degradation and maltose degradation to produce Glc. *B*, α-amylase exhibits carbohydrate-specific binding activity and binds to *N*-linked glycans of glycoproteins in BBM. Both α-amylase and SI are activated and exist in close proximity to work cooperatively in degrading starch to produce glucose. *Left*, the generated Glc is incorporated into enterocytes via SGLT1 under a medium or low concentration of α-amylase. *Right*, under high concentrations of α-amylase, which will occur for a short time after secretion of pancreatic fluid, α-amylase inhibits the Glc transport of SGLT1. Under this condition, Glc incorporation into enterocytes is stopped to avoid a rapid increase of the blood Glc level and maintain blood sugar homeostasis. Removal of α-amylase recovers the activity of SGLT1. *Amy*, pancreatic α-amylase; *SI*, highly *N*- and *O*-glycosylated sucrose-isomaltase; *GT*, SGLT1, which is *N*-glycosylated at one site and forms a homotetramer. BBM is located at a luminal surface of the duodenum and consists of highly glycosylated proteins and lipids.

GNA, which has specificity to α1–3- and α1–6-linked high mannose structures (Fig. 9*C*).

The inhibition of binding of PPA to SI or SGLT1 by mannan (Fig. 5, *C* and *D*) and the neutralization by GNA for inhibition of SGLT1 activity by PPA (Fig. 9*C*) were incomplete. This is attributable to the fact that PPA binds to ligand glycoproteins in BBM at much higher affinity than that to mannan and to the differences in specificity between PPA and GNA, which coincides with the fact that all GNA-positive bands in BBM were not purified on a PPA column (Fig. 4), including the possibility that not only carbohydrate-specific interaction but also protein-protein interaction is involved in the binding of PPA to ligands in BBM.

Starch Degradation by α-Amylase Is Enhanced by Binding to BBM—PPA was found to be activated by interaction with BBMV (Fig. 7). The starch degradation was measured by the release of reducing sugars. Because BBMV contained PPA that had been incorporated into enterocytes from pancreatic fluid and enzymes, such as SI and glycoamylase, which are involved in the digestion of sugars, they were inactivated by heat treatment before measurement. The starch-degrading activity of PPA was enhanced up to 240% in the presence of heat-treated BBMV at a 100-fold (w/w) amount of PPA, which would be attributable to the allosteric activation of PPA by binding to *N*-glycosylated glycoproteins in BBMV as suggested for activation by glycoprotein (7). The direct result of the interaction

between PPA and BBM was shown to be a marked activation of starch degradation, but this study proposes something of greater significance. The interaction of α-amylase with BBM spatially links endo-starch hydrolysis and maltooligosaccharide metabolism to the apical surface of enterocytes (Fig. 12*B*), which increases the catalytic efficiency of starch metabolism because among the glycoprotein ligands for α-amylase identified in BBM were SI and SGLT-1, which are significantly relevant to the assimilation of Glc. Therefore, we focused on the effects of PPA binding on the activities of SI and SGLT1.

Functional Changes of SI and SGLT1 Caused by PPA—SI is a highly *N*- and *O*-glycosylated intestinal BBM protein (39) and is an integral protein composed of two subunits (49), sucrase and isomaltase. SI is sorted with high consistency to the apical membrane via *O*-linked glycans (43). In this study, maltose digestion in BBM was enhanced by PPA but not by ConA, whereas sucrose digestion in BBM was decreased slightly by ConA but not by PPA. The differential effects of PPA and ConA would be attributable to the difference in their oligosaccharide specificities (*i.e.* PPA binds to *N*-glycans, especially high Man types, but not to sialylated complex types at neutral pH) (7). In contrast, ConA binds to high Man-type and biantennary complex-type *N*-glycans at neutral pH. Although ConA, GNA, and *M. amurensis* mitogen did not inhibit the enhancement of SI by PPA, mannan did (data not shown); therefore, the enhancement of SI activity by PPA is considered to depend on carbohydrate-specific interactions. It has been reported that sucrose absorption via BBM was lowered by ConA, suggesting the possibility that SI activity is controlled through the glycan (50). The result shown in Fig. 8*B* is related to this observation. The up-regulation of maltose digestion of SI by PPA would significantly promote Glc production from starch when combined with the activation of PPA at the BBM.

SGLT1 (*SLC5A1*) is the main apical transporter for active Glc uptake in epithelial cells of the small intestine (22). A single *N*-glycosylation site is utilized at Asn-248 (51). Previously, it was reported that the glycosylation of SGLT1 is not necessary for transport of Glc because deglycosylation of BBMV (52) and deletion of potential *N*-glycosylation sites by mutation did not reduce the Glc transport activity of SGLT1 (38, 51). In this study, unexpectedly, Glc uptake by SGLT1 was almost completely inhibited by PPA, which was attenuated only by a mannose-specific lectin, GNA (Fig. 11). These results imply that PPA specifically inactivated the Glc transport activity of SGLT1 by binding to *N*-glycans. One possibility is that PPA directly binds to the *N*-glycan of SGLT1 and inhibits the action of SGLT1. In this case, PPA may interfere with the cotransportation of Na$^+$/Glc through conformational changes of SGLT1 (53), probably through the steric hindrance caused by PPA. Another possibility is that the interaction between PPA and SGLT1 is indirect, and another glycoprotein component in BBM may mediate the inhibition. Notably, a previous report showed that angiotensin II, which is formed from angiotensin I by angiotensin-converting enzyme, inhibited SGLT1-dependent Glc transport across the BBM (32). Because angiotensin-converting enzyme 2 was identified as one of the PPA ligands in this study (Fig. 3), angiotensin-converting enzyme 2 may be involved in the inhibition of SGLT1 caused by PPA. In our preliminary experiments, biotin-PPA bound to immunoprecipitated SI and SGLT1, and the bindings were almost abolished after *N*-glycosidase F treatment of the glycoproteins, suggesting that PPA can directly bind to SI and SGLT1 (see supplemental Fig. 3). However, after de-*N*-glycosylation of BBMV by *N*-glycosidase F, the inhibition of the Glc uptake by PPA was unchanged by the presence or absence of *N*-glycans of SGLT1, which might suggest an indirect control mechanism of SGLT1 activity by PPA, via some intermediary ligand in BBM (data not shown).

The inhibition of SGLT1 activity by PPA occurred at PPA concentrations of more than 5 μM ($\sim$0.28 mg/ml), which is a substantial concentration in secreted pancreatic fluid. We consider that PPA inhibits SGLT1 activity only when the Glc level in the lumen is high because it occurred when the concentration of PPA increased at BBM after secretion of pancreatic fluid. The high concentration of PPA prevents rapid Glc uptake via SGLT1 so as to avoid a sudden increase of blood Glc, which would be a hitherto unknown natural defense mechanism intrinsic to PPA to maintain Glc homeostasis in the body.

Biological Significance of Other Ligands for α-Amylase—Several other BBM ligands that may interact directly or indirectly with PPA were identified in this study (Fig. 3), all of which were *N*-glycosylated glycoproteins. The expression level of each ligand in BBM may directly affect the relative abundance of ligands purified by affinity chromatography because E1 and E2 gave essentially the same protein bands on SDS-PAGE (Fig. 3). Therefore, ligands identified from only *lane E1* must not be neglected. We classified the identified ligands into three groups and focused on SI and SGLT1 in group 1 in this study because they are directly involved in Glc digestion and absorption and are stably expressed in BBM. Other ligands may have significant effects by interacting with PPA through their glycans but were not investigated further. The PPA ligands identified in this study included several aminopeptidases (classified as group 2) and the endocytotic recycling proteins (group 3). One possible function for other PPA ligands is to eliminate bound PPA from the apical surface of enterocytes, which is necessary to release the inhibition of SGLT1 by a high concentration of PPA (Fig. 11). It might be caused by degradation of PPA via the action of aminopepetidases (group 2) or by incorporation of PPA into the enterocytes via the binding with the group 3 ligands and endocytosis of the PPA complex. The binding of PPA with those ligands at BBM may be related to the end of the SGLT1 inhibition caused by PPA binding (54). Because the secretion of pancreatic α-amylase is controlled after feeding, the inhibition of Glc incorporation caused by binding of PPA to SGLT1 and the end of the inhibition by removal of PPA must be repeated at the luminal side of the intestine.

Combining previous reports and the PPA property found in this study, we hypothesize that the BBM ligands contribute to at least one of the three following functions: 1) assimilation of Glc by affecting PPA enzymatic activity, 2) degradation of PPA, and 3) internalization and transcytosis of PPA (54). We focused on the first function in this study and will try to clarify the second and third in the future.

Comparison between Carbohydrate Binding Activities of PPA and recHPA—Previously, we reported that the carbohydrate binding of PPA was not observed in α-amylases from human saliva, wheat, and fungus (7). Therefore, whether PPA and HPA share a common carbohydrate binding activity became one of our major concerns in order to determine if this property is unique to mammalian pancreatic α-amylases. In this study, recHPA exhibited carbohydrate binding activities with a specificity essentially equal to that of PPA and recHPA (Fig. 11). Therefore, the biological significance of the carbohydrate-specific interaction of PPA with BBM will also apply to HPA.

Conclusion—This study showed that PPA interacts with the *N*-glycans of glycoproteins to bind to the duodenal BBM and to maximize the catalytic activity to digest starch and produce Glc in cooperation with SI in the lumen. Furthermore, PPA at high concentrations in the physiological range inhibited Glc absorption of enterocytes via SGLT1, which would contribute to maintenance of the blood Glc homeostasis.

REFERENCES

1. Ishikawa, K., Matsui, I., Kobayashi, S., Nakatani, H., and Honda, K. (1993) Substrate recognition at the binding site in mammalian pancreatic α-amylases. *Biochemistry* **32,** 6259–6265
2. Gupta, R., Jaswal, V. M., and Meenu Mahmood, A. (1992) Intestinal epithelial cell surface glycosylation in mice. I. Effect of high protein diet. *Ann. Nutr. Metab.* **36,** 288–295
3. Pusztai, A., Ewen, S. W., Grant, G., Peumans, W. J., Van Damme, E. J., Coates, M. E., and Bardocz, S. (1995) Lectins and also bacteria modify the glycosylation of gut surface receptors in the rat. *Glycoconj. J.* **12,** 22–35
4. Van Halbeek, H., Gerwig, G. J., Vliegenthart, J. F., Smits, H. L., Van Kerkhof, P. J., and Kramer, M. F. (1983) Terminal α (1→4)-linked *N*-acetylglucosamine. A characteristic constituent of duodenal-gland mucous glycoproteins in rat and pig. A high resolution ¹H NMR study. *Biochim. Biophys. Acta* **747,** 107–116
5. Smits, H. L., and Kramer, M. F. (1984) Human duodenal gland (Brunner's gland) mucus glycoprotein analysis. *Arch. Biochem. Biophys.* **228,** 64–70
6. Roth, J. (1993) Cellular sialoglycoconjugates. A histochemical perspective. *Histochem. J.* **25,** 687–710
7. Matsushita, H., Takenaka, M., and Ogawa, H. (2002) Porcine pancreatic α-amylase shows binding activity toward *N*-linked oligosaccharides of glycoproteins. *J. Biol. Chem.* **277,** 4680–4686
8. Takekawa, H., Ina, C., Sato, R., Toma, K., and Ogawa, H. (2006) Novel carbohydrate-binding activity of pancreatic trypsins to *N*-linked glycans of glycoproteins. *J. Biol. Chem.* **281,** 8528–8538
9. Brayer, G. D., Sidhu, G., Maurus, R., Rydberg, E. H., Braun, C., Wang, Y., Nguyen, N. T., Overall, C. M., and Withers, S. G. (2000) Subsite mapping of the human pancreatic α-amylase active site through structural, kinetic, and mutagenesis techniques. *Biochemistry* **39,** 4778–4791
10. Ueno, M., Ogawa, H., Matsumoto, I., and Seno, N. (1991) A novel mannose-specific and sugar specifically aggregatable lectin from the bark of the Japanese pagoda tree (*Sophora japonica*). *J. Biol. Chem.* **266,** 3146–3153
11. Ueda, H., Fukushima, H., Hatanaka, Y., and Ogawa, H. (2004) Solubility-insolubility interconversion of sophoragrin, a mannose/glucose-specific lectin in *Sophora japonica* (Japanese pagoda tree) bark, regulated by the sugar-specific interaction. *Biochem. J.* **382,** 821–829
12. Kessler, M., Acuto, O., Storelli, C., Murer, H., Müller, M., and Semenza, G. (1978) A modified procedure for the rapid preparation of efficiently transporting vesicles from small intestinal brush border membranes. Their use in investigating some properties of D-glucose and choline transport systems. *Biochim. Biophys. Acta* **506,** 136–154
13. Hugon, J., and Borgers, M. (1966) Ultrastructural localization of alkaline phosphatase activity in the absorbing cells of the duodenum of mouse. *J. Histochem. Cytochem.* **14,** 629–640
14. Harlow, E., and Lane, D. (1988) *Antibodies: A Laboratory Manual*, Cold Spring Harbor Laboratory Press, Cold Spring Harbor, NY
15. Nakagawa, K., Nakamura, K., Haishima, Y., Yamagami, M., Saito, K., Sakagami, H., and Ogawa, H. (2009) Pseudoproteoglycan (pseudoPG) probes that simulate PG macromolecular structure for screening and isolation of PG-binding proteins. *Glycoconj. J.* **26,** 1007–1017
16. Dahlqvist, A. (1968) Assay of intestinal disaccharidases. *Anal. Biochem.* **22,** 99–107
17. Takahashi, K., Masuda, S., Nakamura, N., Saito, H., Futami, T., Doi, T., and Inui, K. (2001) Up-regulation of H⁺-peptide cotransporter PEPT2 in rat remnant kidney. *Am. J. Physiol. Renal Physiol.* **281,** F1109–F1116
18. Shiosaki, K., Takata, K., Omichi, K., Tomita, N., Horii, A., Ogawa, M., and Matsubara, K. (1990) Identification of a novel α-amylase by expression of a newly cloned human amy3 cDNA in yeast. *Gene* **89,** 253–258
19. Fornstedt, N., and Porath, J. (1975) Characterization studies on a new lectin found in seeds of *Vicia ervilia. FEBS Lett.* **57,** 187–191
20. Mellitzer, G., Beucher, A., Lobstein, V., Michel, P., Robine, S., Kedinger, M., and Gradwohl, G. (2010) Loss of enteroendocrine cells in mice alters lipid absorption and glucose homeostasis and impairs postnatal survival. *J. Clin. Invest.* **120,** 1708–1721
21. Stevens, B. R., Fernandez, A., Hirayama, B., Wright, E. M., and Kempner, E. S. (1990) Intestinal brush border membrane Na⁺/glucose cotransporter functions *in situ* as a homotetramer. *Proc. Natl. Acad. Sci. U.S.A.* **87,** 1456–1460
22. Hediger, M. A., Coady, M. J., Ikeda, T. S., and Wright, E. M. (1987) Expression cloning and cDNA sequencing of the Na⁺/glucose co-transporter. *Nature* **330,** 379–381
23. Sjöström, H., Norén, O., Christiansen, L., Wacker, H., and Semenza, G. (1980) A fully active, two-active site, single-chain sucrase-isomaltase from pig small intestine. Implications for the biosynthesis of a mammalian integral stalked membrane protein. *J. Biol. Chem.* **255,** 11332–11338
24. Danielsen, E. M., Hansen, G. H., and Niels-Christiansen, L. L. (1995) Localization and biosynthesis of aminopeptidase N in pig fetal small intestine. *Gastroenterology* **109,** 1039–1050
25. Fan, H., Meng, W., Kilian, C., Grams, S., and Reutter, W. (1997) Domain-specific *N*-glycosylation of the membrane glycoprotein dipeptidylpeptidase IV (CD26) influences its subcellular trafficking, biological stability, enzyme activity, and protein folding. *Eur. J. Biochem.* **246,** 243–251
26. Khatri, I. A., Wang, R., and Forstner, J. F. (2003) SEA (sea urchin sperm protein, enterokinase, and agrin)-module cleavage, association of fragments, and membrane targeting of rat intestinal mucin Muc3. *Biochem. J.* **372,** 263–270
27. Kenan, N., Larsson, A., Axelsson, O., and Helander, A. (2011) Changes in transferrin glycosylation during pregnancy may lead to false-positive carbohydrate-deficient transferrin (CDT) results in testing for riskful alcohol consumption. *Clin. Chim. Acta* **412,** 129–133
28. Georgieff, M. K., Petry, C. D., Mills, M. M., McKay, H., and Wobken, J. D. (1997) Increased *N*-glycosylation and reduced transferrin-binding capacity of transferrin receptor isolated from placentae of diabetic women. *Placenta* **18,** 563–568
29. Hayes, G. R., Williams, A., Costello, C. E., Enns, C. A., and Lucas, J. J. (1995) The critical glycosylation site of human transferrin receptor contains a high mannose oligosaccharide. *Glycobiology* **5,** 227–232
30. Le Varlet, B., Staquet, M. J., Dezutter-Dambuyant, C., Gaucherand, M., and Schmitt, D. (1991) Expression and endocytosis of integrin VLA receptors for collagen, fibronectin and laminin by normal human keratinocytes. *J. Dermatol. Sci.* **2,** 287–299
31. Russell, M. R., Nickerson, D. P., and Odorizzi, G. (2006) Molecular mechanisms of late endosome morphology, identity and sorting. *Curr. Opin. Cell Biol.* **18,** 422–428
32. Wong, T. P., Debnam, E. S., and Leung, P. S. (2007) Involvement of an enterocyte renin-angiotensin system in the local control of SGLT1-dependent glucose uptake across the rat small intestinal brush border membrane. *J. Physiol.* **584,** 613–623
33. Gordon, K., Redelinghuys, P., Schwager, S. L., Ehlers, M. R., Papageorgiou,

A. C., Natesh, R., Acharya, K. R., and Sturrock, E. D. (2003) Deglycosylation, processing, and crystallization of human testis angiotensin-converting enzyme. *Biochem. J.* **371,** 437–442

34. Watermeyer, J. M., Sewell, B. T., Schwager, S. L., Natesh, R., Corradi, H. R., Acharya, K. R., and Sturrock, E. D. (2006) Structure of testis ACE glycosylation mutants and evidence for conserved domain movement. *Biochemistry* **45,** 12654–12663

35. Tokhtaeva, E., Munson, K., Sachs, G., and Vagin, O. (2010) *N*-Glycan-dependent quality control of the Na,K-ATPase β_2 subunit. *Biochemistry* **49,** 3116–3128

36. Aertgeerts, K., Ye, S., Tennant, M. G., Kraus, M. L., Rogers, J., Sang, B. C., Skene, R. J., Webb, D. R., and Prasad, G. S. (2004) Crystal structure of human dipeptidyl peptidase IV in complex with a decapeptide reveals details on substrate specificity and tetrahedral intermediate formation. *Protein Sci.* **13,** 412–421

37. Aït-Slimane, T., Galmes, R., Trugnan, G., and Maurice, M. (2009) Basolateral internalization of GPI-anchored proteins occurs via a clathrin-independent flotillin-dependent pathway in polarized hepatic cells. *Mol. Biol. Cell* **20,** 3792–3800

38. Wright, E. M., Turk, E., Hager, K., Lescale-Matys, L., Hirayama, B., Supplisson, S., and Loo, D. D. (1992) The Na$^+$/glucose cotransporter (SGLT1). *Acta Physiol. Scand. Suppl.* **607,** 201–207

39. Hunziker, W., Spiess, M., Semenza, G., and Lodish, H. F. (1986) The sucrase-isomaltase complex. Primary structure, membrane orientation, and evolution of a stalked, intrinsic brush border protein. *Cell* **46,** 227–234

40. Gallicchio, M. A., and Bach, L. A. (2010) Advanced glycation end products inhibit Na$^+$ K$^+$ ATPase in proximal tubule epithelial cells. Role of cytosolic phospholipase A2α and phosphatidylinositol 4-phosphate 5-kinase gamma. *Biochim. Biophys. Acta* **1803,** 919–930

41. Tokhtaeva, E., Sachs, G., and Vagin, O. (2010) Diverse pathways for maturation of the Na,K-ATPase β1 and β2 subunits in the endoplasmic reticulum of Madin-Darby canine kidney cells. *J. Biol. Chem.* **285,** 39289–39302

42. Radoshitzky, S. R., Kuhn, J. H., Spiropoulou, C. F., Albariño, C. G., Nguyen, D. P., Salazar-Bravo, J., Dorfman, T., Lee, A. S., Wang, E., Ross, S. R., Choe, H., and Farzan, M. (2008) Receptor determinants of zoonotic transmission of New World hemorrhagic fever arenaviruses. *Proc. Natl. Acad. Sci. U.S.A.* **105,** 2664–2669

43. Naim, H. Y., Joberty, G., Alfalah, M., and Jacob, R. (1999) Temporal association of the *N*- and *O*-linked glycosylation events and their implication in the polarized sorting of intestinal brush border sucrase-isomaltase, aminopeptidase N, and dipeptidyl peptidase IV. *J. Biol. Chem.* **274,** 17961–17967

44. Nichols, B. L., Avery, S., Sen, P., Swallow, D. M., Hahn, D., and Sterchi, E. (2003) The maltase-glucoamylase gene. Common ancestry to sucrase-isomaltase with complementary starch digestion activities. *Proc. Natl. Acad. Sci. U.S.A.* **100,** 1432–1437

45. Detel, D., Baticic, L., and Varljen, J. (2008) The influence of age on intestinal dipeptidyl peptidase IV (DPP IV/CD26), disaccharidases, and alkaline phosphatase enzyme activity in C57BL/6 mice. *Exp. Aging Res.* **34,** 49–62

46. Russell, J. R., Young, A. W., and Jorgensen, N. A. (1981) Effect dietary corn starch intake on pancreatic amylase and intestinal maltase and pH in cattle. *J. Anim. Sci.* **52,** 1177–1182

47. Gorrill, A. D., Thomas, J. W., Stewart, W. E., and Morrill, J. L. (1967) Exocrine pancreatic secretion by calves fed soybean and milk protein diets. *J. Nutr.* **92,** 86–92

48. Fukuoka, S. (1992) *Tanpakushitsu Kakusan Koso* **37,** 795–809

49. Brunner, J., Hauser, H., Braun, H., Wilson, K. J., Wacker, H., O'Neill, B., and Semenza, G. (1979) The mode of association of the enzyme complex sucrase-isomaltase with the intestinal brush border membrane. *J. Biol. Chem.* **254,** 1821–1828

50. Rueda, E., León, M., Castañeda, M., Mendez, A., and Michelangeli, C. (2007) Effects of concanavalin A on intestinal brush border enzyme activity in broiler chickens. *Br. Poult. Sci.* **48,** 696–702

51. Hediger, M. A., Mendlein, J., Lee, H. S., and Wright, E. M. (1991) Biosynthesis of the cloned intestinal Na$^+$/glucose cotransporter. *Biochim. Biophys. Acta* **1064,** 360–364

52. Hirayama, B. A., and Wright, E. M. (1992) Glycosylation of the rabbit intestinal brush border Na$^+$/glucose cotransporter. *Biochim. Biophys. Acta* **1103,** 37–44

53. Loo, D. D., Hirayama, B. A., Gallardo, E. M., Lam, J. T., Turk, E., and Wright, E. M. (1998) Conformational changes couple Na$^+$ and glucose transport. *Proc. Natl. Acad. Sci. U.S.A.* **95,** 7789–7794

54. Cloutier, M., Gingras, D., and Bendayan, M. (2006) Internalization and transcytosis of pancreatic enzymes by the intestinal mucosa. *J. Histochem. Cytochem.* **54,** 781–794